Appl. Phys. B 66, 201–205 (1998)

Applied Physics B
Lasers
and Optics

Visible and infrared dispersion of the refractive indices in periodically poled and single domain Nd:Mg:LiNbO$_3$ crystals

G.K. Kitaeva, I.I. Naumova, A.A. Mikhailovsky, P.S. Losevsky, A.N. Penin

Department of Physics, Moscow State University, 119899, Moscow, Russia
(Fax: +7-95/939-3113, E-mail: postmast@spr.phys.msu.su)

Received: 29 January 1997/Revised version: 10 July 1997

Abstract. Dispersion characteristics of bulk single-domain and periodically poled Nd:Mg:LiNbO$_3$ crystals are measured in the transparency region (with the accuracy ± 0.0002) and for the upper phonon polariton branch (with the accuracy ± 0.003–± 0.05), from 0.44 µm up to 10.5 µm. The method of spontaneous parametric light scattering is used for measurement of the ordinary refractive index dispersion in the mid-infrared region and for determination of the domain grating period $d = 5.6 \pm 0.2$ µm in the periodically-poled crystal.

PACS: 78.20.Ci; 77.84.Dy; 42.65.-k

Bulk crystals of doped LiNbO$_3$ are important for a variety of applications using nonlinear optical, ferroelectric and photorefractive effects. Nonlinear optical devices, such as second-harmonic generators and optical parametric oscillators, require crystals of high optical quality. To reduce photorefractive damage, LiNbO$_3$ needs to be doped with magnesium oxide (MgO). Bryan et al. [1] reported that the resistance to optical damage in Mg:LiNbO$_3$ is due to a significant increase in the photoconductivity. Periodic distribution of the impurity concentration provides the periodic character of the crystal domain structure. Such periodically poled crystals are used for quasi-phase matching.

Two approaches are implemented now to satisfy phase matching conditions in nonlinear crystal devices. The more common one is based on the crystal birefringence [2]. However, sometimes it does not allow one to make use of certain high-value components of the nonlinear susceptibility tensor (such as χ_{zzz} in LiNbO$_3$). Quasi-phase matching is an alternative technique for compensation of the phase velocity dispersion in frequency-conversion applications [3, 4]. Under this type of phase matching, the nonlinear coefficient should be modulated with the period $\Lambda = 2ml_c$, where $m = 1, 2, 3, \ldots$ and l_c is the coherence length of the interaction (mostly about several microns for LiNbO$_3$ crystals). Periodic reversals of the spontaneous polarization $\boldsymbol{P}_S$ in LiNbO$_3$ correlate with the reversals of the sign of the nonlinear coefficient. The superlattice acts as the linear refractive index grating and as the nonlinear grating of the quadratic susceptibility [4]. In both cases, one needs to know the refractive indices to an accuracy of 10^{-4} in order to determine the orientation of wavevectors to an accuracy of 1°. At the same time, the presence of doping agents changes essentially the optical characteristics of LiNbO$_3$ crystals [5]. Application of nonlinear frequency conversion devices demands accurate data on the refractive indices dispersion of doped LiNbO$_3$. Also, these data can be used to solve the inverse problem of developing optical methods to characterize the composition and homogeneity of lithium niobate crystals [6].

Dispersion of the refractive indices has been measured by a number of authors [7–12] in homogeneous LiNbO$_3$ crystals of different composition without doping agents. For several magnesium and yttrium doped bulk LiNbO$_3$ crystals, the dispersion was studied in [5]. In [13], the generalized Sellmeier equation was obtained for the wavelength range 400 to 1200 nm with an account of the defect structure of Li-deficient and Mg-doped LiNbO$_3$ crystals. In the present work, we report the results on the dispersion of refractive indices in double Nd- and Mg-doped single crystals in the visible and IR region up to l0.5 µm.

1 Characteristics of the crystals

Bulk Nd:Mg:LiNbO$_3$ single crystals were grown using the Czochralski method. The starting material was close to congruently melting composition with the ratio $\mathrm{Li/Nb} = 0.942$. It was prepared from the high-purity components (Nb$_2$O$_5$ and Li$_2$CO$_3$) by synthesis at 1050 °C for 20 hours. The crystals were grown in a platinum crucible under air, normal to the $(01\bar{1}2)$ face [14]. As a rule, the upper part of the crystal boule grown by this method has no multiply-domained structure. This structure appears in the lower part of the crystal. We suppose that this is a result of the concurrent influences of the two axial gradients: the gradient of the temperature, which has the same sign in all parts of the crystal during the growth, and the gradient of the impurity concentration, which periodically changes its sign along the growth direction and leads to the appearence of domains with oppositely oriented $\boldsymbol{P}_S$ vectors. The first factor is more efficient in the upper part of the crystal and, under proper conditions of the growth procedure, it can cause the formation of a single-domain area there. The multiply-domained structure appears in the region where the influence of the local gradient of impurity concentration is more effective than the influence of the temperature gradient. The structure of the grown crystal boule also varies along the transverse direction. The most important part is the central part, where the orientation of the domain walls coincide with the $(01\bar{1}2)$ face. Here, the face of the growth front gives rise to a system of lamellar domains, which are thin layers oriented exactly in the $(01\bar{1}2)$ plane, so that the normal to the layers, located in the YZ-plane, is oriented at 57° to the Z-axis. This type of orientation provides a high optical quality of the domain walls, which have small thicknesses and are plane. In the present work, one of the two studied samples was a single-domain crystal element, cut from the upper part of a boule. The other sample, a multiply-domained sample, had a layer-type domain structure of face-type with a high degree of space periodicity; it was cut from the central area of the lower part of another boule.

Distribution of the impurities was studied by means of wave dispersive X-ray microanalysis. Measurements of the distribution of the impurity mass concentration were made using Camebax SX-50. The relative experimental error was about 2% for the measurement of Nd-concentration, and about 1% for the measurement of Mg-concentration. According to the X-ray microanalysis, the average value of Mg-element concentration was 0.33 mass% (2.05 mol%) in the multiply-domained crystal and 0.41 mass% (2.56 mol%) in the single-domain crystal; the average Nd-element concentration was 0.31–0.32 mass% (0.33–0.34 mol%) in both crystals. The maximum variation of the Nd-concentration (0.16 mass%) throughout the studied areas in both crystals was several times larger than the maximum variations of the Mg-concentration. Recently, it has been reported that there is a good agreement between the period of the regular domain structure and the period of the modulation of the rare-earth element concentration in Eu:Mg:$LiNbO_3$ [15] and in Nd:Mg:$LiNbO_3$ [16].

Periodic spatial variation of the impurity concentration causes periodic spatial variation of the extraordinary refractive index of the crystal. The linear grating in the crystals with the periodic variation of impurity concentration was studied by means of the optical Bragg-diffraction method. In single-domain crystals the linear grating is close to sinusoidal. In multiply-domained crystals, the influence of the bounded carriers localized on the domain walls causes noticeable changes in the space distribution of the refractive index. It was shown in [17] by the analysis of 15 orders of optical linear diffraction, that spatial variation of the extraordinary refractive index in multiply-domained crystals is far from being sinusoidal and consists of sharp peaks of the order of $\Delta n_e \approx 5 \times 10^{-5}$ with thickness 0.2–0.5 μm, localized on the domain walls.

2 Dispersion of refractive indices in the visible range

We have measured the dispersion characteristics of the ordinary (n_o) and extraordinary (n_e) refractive indices of the crystals in the visible and near-infrared ranges at room temperature by the prism method, using a goniospectrometer. The refractive indices were determined in the infrared range at a wavelength of 1.06 μm with the help of an image converting visualizer. The absolute error did not exceed ±0.0002. The results of measurements at different wavelengths are presented in the Table 1. The values of n_o and n_e are averaged over spatial areas that are large in comparison with the period of the linear and nonlinear gratings. The values of the refractive indices were the same within the limits of the measurement accuracy both for the parts of crystals with periodic linear gratings and for those without them. The dispersion characteristics $n_o(\lambda)$ and $n_e(\lambda)$ can be represented as

$$n^2 = A - B/(C - \lambda^2) - D\lambda^2 \tag{1}$$

with the coefficients A, B, C and D differing slightly in each sample. The values of the Sellmeier coefficients calculated for the doped crystals and undoped congruent $LiNbO_3$ are given in Table 2 (the wavelength λ is given in nanometres). The mean accuracy of the values of refractive indices calculated by this Sellmeier formula is near ±0.0003.

Figure 1 demonstrates the deviations $\Delta n_{o,e} = n_{o,e} - n^0_{o,e}$ of the refractive indices $n_{o,e}$ for both of the investigated crystals from the refractive indices $n^0_{o,e}$ of the undoped congruent $LiNbO_3$ at different wavelengths. The data for undoped congruent $LiNbO_3$ were taken from [12]. For comparison, we also show the results of [13] on single-doped homogeneous Mg:$LiNbO_3$ crystals with the same concentration of Mg. As one can see from Fig. 1, the main qualitative differences in the spectral behaviour of deviations $\Delta n_{o,e}$ are located near the

Table 1. Refractive indices at visible and near IR ranges

Wavelength (nm)	Polarization	Multiply-domained crystal $N_{Mg} = 2.05$ mol% $N_{Nd} = 0.33$ mol%	Single-domain crystal $N_{Mg} = 2.56$ mol% $N_{Nd} = 0.34$ mol%
441.6	o	2.3854	2.3838
	e	2.2856	2.2798
488	o	2.347	2.3457
	e	2.2504	2.2479
546.07	o	2.315	2.314
	e	2.2233	2.2213
577	o	2.3023	2.3012
	e	2.2122	2.2103
632.8	o	2.285	2.2842
	e	2.1974	2.1958
676.4	o	2.2746	2.2735
	e	2.1886	2.1868
1064	o	2.2303	2.23
	e	2.1506	2.1495

Table 2. Sellmeier coefficients for doped crystals and undoped congruent $LiNbO_3$

Crystal no.	Polarization	A	$10^{-4}B$	$10^{-4}C$	$10^8 D$
Multiply-domained crystal					
$N_{Mg} = 2.05$ mol%	o	4.9109	11.3813	5.0311	3.6992
$N_{Nd} = 0.33$ mol%	e	4.5999	8.3609	6.2881	4.6900
Single-domain crystal					
$N_{Mg} = 2.56$ mol%	o	4.9001	11.5737	4.8182	3.0052
$N_{Nd} = 0.34$ mol%	e	4.5581	9.7078	4.4267	2.3873

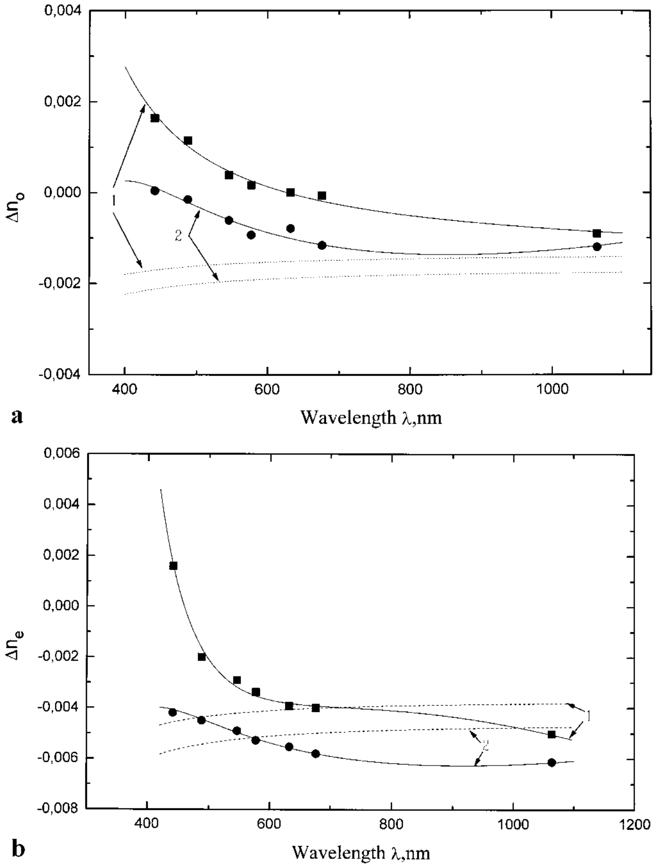

Fig. 1a,b. Spectral dependencies of the deviations $\Delta n_{\mathrm{o,e}} = n_{\mathrm{o,e}} - n^0_{\mathrm{o,e}}$ of refractive indices (**a** ordinary, **b** extraordinary) of the doped Nd:Mg:LiNbO$_3$ crystals ($n_{\mathrm{o,e}}$) from that of the undoped one ($n^0_{\mathrm{o,e}}$). Squares denote experimental data obtained for the multiply-domained crystal (No.1), circles denote the data obtained for the single-domain one (No.2). Solid curves show differences between the Sellmeier functions taken from [12] for $n^0_{\mathrm{o,e}}$ and those calculated on the basis of Table 2 for $n_{\mathrm{o,e}}$. Dashed curves present analogous dependencies for the Mg:LiNbO$_3$ crystals with the same Mg-content (Sellmeier functions were taken from [13])

blue end of the transparency range. In this range, the additional doping by Nd makes the values of the refractive indices to increase, in contrast to the influence of Mg, which leads to a decrease in $n_{\mathrm{o,e}}$. The effect of Nd-doping on $n_{\mathrm{o,e}}$ decreases at higher wavelengths. It is difficult to compare qualitatively the results of [13] with ours and to extract the spectral dependence of the influence of Nd on $n_{\mathrm{o,e}}$, since the errors of the Mg-content determination are too large. Another reason is a possible difference in the starting materials taken for the crystal growth in the two works. The next qualitative conclusion can be made by comparing our results obtained by fitting the experimental data by the Sellmeier formula. While dispersion curves for n_{o} have a similar character for the multiply-domained crystal and for the single-domain crystal, there are differences in the spectral behaviour of the extraordinary refractive indices of both studied crystals. Note that the measured $n_{\mathrm{o,e}}$ are the average values, characterizing the optical response of the crystal areas that include a large number of domain layers. As is known from optical Bragg-diffraction analysis [17], the spatial distribution of n_{e} in the crystals with the growth layers is sensitive to the existence of the domain grating. According to our results, it seems that the spectral behaviour of the averaged extraordinary refractive index is also sensitive to the periodic domain structure.

3 Refractive index dispersion for the upper polariton branch and period of regular domain structure

In order to study the dispersion characteristics of the crystals in the mid-infrared range, we used the method of spontaneous parametric scattering of light [18] (SPS). This method enables one to measure the real and imaginary parts of the dielectric constant in spectral regions where crystal absorption is large: in the region of phonon polaritons and at the upper phonon polariton branch [19]. In contrast to direct methods, based on the treatment of IR reflectivity and transparency spectra [20], information about IR optical characteristics is converted into the visible range. Dispersion characteristics are determined from two-dimensional frequency-angular distribution of the scattered light intensity in the scheme of near-forward Raman scattering [21].

We have employed the SPS method for the measurement of the ordinary refractive index of the Nd:Mg:LiNbO$_3$ crystals in the spectral region 2.5–10.5 μm including the upper polariton branch. Radiation of the Ar-laser at the wavelength of 488 nm was used as a pump beam. The scattering was observed under the nonlinear interaction of ooe type in the basic crystal planes, including the crystal Z-axis: the polariton and signal waves were ordinarily polarized in the direction normal to the scattering plane, the pump wave was extraordinarily polarized in the scattering plane. The scattered radiation passed through the registration system, including analyser, lens system and spectrograph and was registered by a photographic film. Spectral selection of the scattered radiation was made by a spectrograph. The lens system was arranged to make the angular selection of the scattered radiation. The scattered signal light passed through the analyser and was focused by the lens system on to the spectrograph slit. The crystal (from one side) and the slit (from the other side) were placed in the focal planes of the lens system, the optical axis of the lens system coincided with the direction of the pump. The spectral components of the scattered radiation formed a ring in the plane of the slit, the radius being proportional to tg θ_{s}, where θ_{s} was the angle of declination from the direction of the pump. The slit cut from these rings the radiation which lay in the plane given by the slit and the direction of the pump propagation. At the exit of the spectrograph camera, the radiation was focused at a distance from the spectrograph optical axis proportional to the radius of the ring at the entrance slit. The two-dimensional distribution of signal intensity in coordinates of signal wavelength λ_{s} vs angle θ_{s} was registered by a photographic film at the exit of the spectrograph.

In the process of SPS, the pump photon of frequency ω_{L} decays into two particles: a polariton of some frequency ω_{p} and a signal photon of frequency ω_{s}, equal to

$$\omega_{\mathrm{s}} = \omega_{\mathrm{L}} - \omega_{\mathrm{p}} \tag{2}$$

The intensity of the signal is maximized when the phase matching conditions are satisfied:

$$\boldsymbol{k}_{\mathrm{s}} = \boldsymbol{k}_{\mathrm{L}} - \boldsymbol{k}_{\mathrm{p}} \tag{3}$$

where $\boldsymbol{k}_\mathrm{s}$, $\boldsymbol{k}_\mathrm{L}$ and $\boldsymbol{k}_\mathrm{p}$ are the wavevectors of signal, laser and polariton waves, respectively. When the shift between polariton and phonon frequencies is large in comparison with the phonon damping constant, the scattering occurs due to the second-order optical susceptibility only. In the vicinity of a phonon resonance, there is an additional contribution to the scattering intensity from the Raman scattering tensor. When the polariton frequency is larger than all the phonon frequencies, the scattering takes place at the upper polariton branch. In this case, it is known as spontaneous parametric down-conversion, a source of quantum noise in optical parametric oscillators [22].

Figure 2 shows examples of experimental SPS spectra obtained for the single domain (a) and periodically-poled multiply-domained (b) crystals. The experimental spectra also include the signal from 180°-Raman scattering by phonon modes, reflected from the input crystal surface; in contrast to SPS curves, this scattering occurs at constant frequencies and at all angles under registration.

The standard treatment of two-dimensional SPS spectra requires the determination of the angles $\theta_{\mathrm{S}0}$, at which the signal intensity is maximum, for each signal wavelength λ_s. The pump and signal frequencies are located in the region of the crystal transparency. The SPS method provides a measurement of the crystal refractive indices and absorption coefficients at polariton frequencies, if the values of the crystal refractive indices at the signal and pump frequencies are known. For a given type of interaction, the SPS spectra of homogeneous crystals consist of single tuning curves $\theta_{\mathrm{S}0}(\lambda_\mathrm{S})$, which are described by relations (2) and (3). One can determine the effective values of the refractive index of a crystal at corresponding polariton frequency by substituting the values of θ_S measured at each signal wavelength λ_S into (2) and (3).

In the case of periodically poled crystals, there can be a set of tuning curves in the same spectral region [23]. Their origin is due to the periodic modulation of the second-order susceptibility of a crystal caused by the periodic reversals of the spontaneous polarization $\boldsymbol{P}_\mathrm{S}$ at domain boundaries. Each harmonic χ_m in the Fourier series of the second-order susceptibility provides parametric scattering into the m-th order maximum of the nonlinear diffraction. The direction of the signal propagation in the m-th order maximum is described by the phase-matching condition [23]:

$$\boldsymbol{k}_\mathrm{S} = \boldsymbol{k}_\mathrm{L} - \boldsymbol{k}_\mathrm{p} - \boldsymbol{q}_\mathrm{m} \tag{4}$$

where $\boldsymbol{q}_\mathrm{m} = 2\pi m \boldsymbol{n}/d$ is the wavevector of the inverse nonlinear superlattice, d is the space period of reversals of the spontaneous polarization P_S at the domain boundaries and $\boldsymbol{n}$ is the unit vector normal to the domain layers.

The spectral dependencies of the ordinary refractive index obtained by the SPS-method are presented in Fig. 3. The accuracy of the measurements depends on the spectral range. At the upper polariton branch it decreases with the wavelength. The absolute error is maximum ($\Delta n_\mathrm{o} = \pm 0.05$) in the spectral range 10.5 μm to ≈ 8.5 μm where the value $|\mathrm{d}n/\mathrm{d}\lambda|$ is also maximum. It decreases down to ± 0.003 as the wavelength approaches the transparency region and the value of $|\mathrm{d}n/\mathrm{d}\lambda|$ decreases. The absolute error of the frequency measurement was determined by the spectral linewidth of the spectrograph entrance slit. In our case it was the same over the whole investigated IR range: $\Delta\omega = \pm 10\,\mathrm{cm}^{-1}$. One can see from Fig. 3, that the dispersion curves $n_\mathrm{o}(\omega)$ for the investigated differently doped crystals do not differ from each other in the limits of accuracy of measurement. So, comparing the differences between the refractive indices in the visible range and the experimental error of measurement in the IR range, we can conclude that the differences in dispersion curves do not increase when the wavelength shifts from the visible range to the infrared range, at least up to 5 μm.

The mean values of the refractive index of the multiply-domained crystal were measured on the basis of the unshifted tuning curves, corresponding to the scattering into a zeroth order maximum of the nonlinear diffraction. At the same time, the phase-matching conditions (4) and the profile of the nonlinear grating enabled us to observe the scattering into one of the first order maxima of the nonlinear diffraction ($m = -1$). Using the measured values of the polariton refractive index, we have determined the inverse nonlinear superlattice wavevector $\boldsymbol{q}_{-1}$ and the domain superlattice period

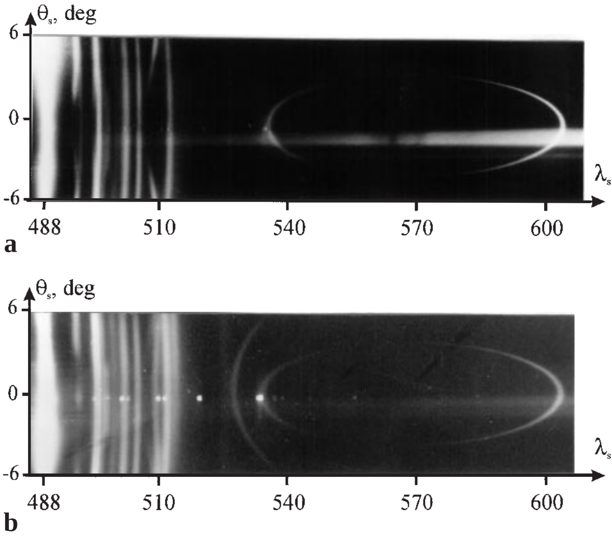

Fig. 2a,b. SPS spectra of the single-domain (**a**) and periodically poled (**b**) Nd:Mg:LiNbO$_3$ crystals. In both cases the angle between the direction of pump incidence and the crystal Z-axis is 47.4°, the input and output crystal surfaces are cut parallel to the growth layers (at the angle of 57° to the Z-axis)

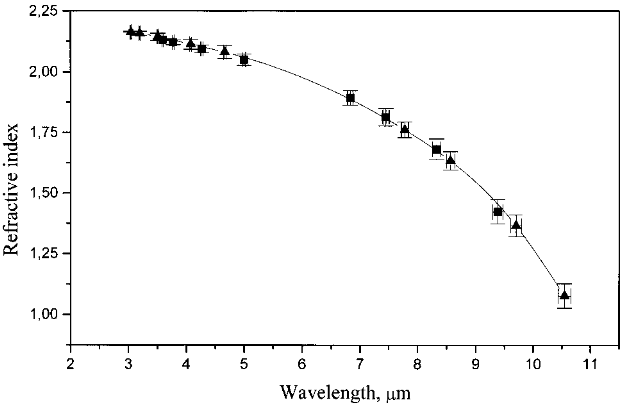

Fig. 3. Dispersion of the ordinary refractive index in the IR range for the Nd:Mg:LiNbO$_3$ crystals. Squares denote the multiply-domained crystal, triangles denote the single-domain one

d. The measured value of the domain superlattice period is $d = 5.6 \pm 0.2\,\mu\text{m}$ for the periodically poled crystal. The values of d determined by this method at the different polariton frequencies coincide within the measurement accuracy. This fact confirms the correctness of our interpretation of the SPS spectra observed in the periodically poled crystal.

4 Summary

The dispersion characteristics of bulk Nd:Mg:LiNbO$_3$ single crystals were studied in the visible and infrared ranges. The ordinary and extraordinary refractive indices were measured by the prism method in the range 0.44–1.06 μm, the ordinary refractive indices were measured by the method of spontaneous parametric light scattering in the range 2.5–10.5 μm, including the upper phonon polariton branch.

The effect of nonlinear diffraction was observed under spontaneous parametric scattering in the periodical multiply domained crystal of Nd:Mg:LiNbO$_3$. The value of the domain superlattice period $d = 5.6\,\mu\text{m}$ was determined from angle dependencies of the scattered light intensity with the accuracy of $\pm 0.2\,\mu\text{m}$.

Acknowledgements. The authors are grateful to S.P. Kulik and M.V. Chekhova for several useful discussions. This work was supported by the Russian Foundation of Basic Research (Grant No 96-02-16336a).

References

1. D.A. Bryan, R. Gerson, H.E. Tomaschke: Appl. Phys. Lett. **44**, 847 (1984)
2. G.D. Boyd et al.: Appl. Phys. Lett. **5**, 234 (1964)
3. J.A. Armstrong et al.: Phys. Rev. **127**, 1918 (1962)
4. M.M. Fejer et al.: IEEE J. Quantum Electron. **28**, 2631 (1992)
5. A.L. Aleksandrovskii et al.: Sov. J. Quantum Electron. **21**(2), 225 (1991)
6. M. Wohlecke et al.: Appl. Phys. B **63**, 323 (1996)
7. D.F. Nelson, R.M. Mikulyak: J. Appl. Phys. **45**, 3688 (1974)
8. D.S. Smith, H.D. Riccius, R.P. Edwin: Opt. Commun. **17**, 332 (1976)
9. M.V. Hobden, J. Warner: Phys. Letts. **22**, 243 (1966)
10. J.G. Bergman et al.: Appl. Phys. Letts. **12**, 92 (1967)
11. G.M. Georgiev et al.: Sov. Phys. Solid State **16**, 2293 (1975)
12. U. Schlarb, K. Betzler: Phys. Rev. B **48**, 15613 (1993)
13. U. Schlarb, K. Betzler: Phys. Rev. B **50**, 751 (1994)
14. I.I. Naumova: Crystallogr. Rep. **39**, Nr.6, 1119 (1994)
15. I.I. Naumova et al.: Ferroelectrics **190**, 107 (1997)
16. I.I. Naumova et al.: J. Cryst. Growth **180**, (1997) - to be published
17. A.L. Aleksandrovsky et al.: Quantum Electron. **26**, 641 (1996)
18. D.N. Klyshko: *Photons and Nonlinear Optics* (Gordon & Breach, 1987)
19. Y.N. Polivanov: Sov. Phys. Usp. **21**, 805 (1978)
20. A.S. Barker, R. Loudon: Phys. Rev. **158**, 433 (1967)
21. M.V. Chekhova, A.N. Penin: J. Raman Spectrosc. **24**, 581 (1993)
22. D.A. Kleinman: Phys. Rev. **174**, 1027 (1968)
23. A.L. Aleksandrovsky et al.: Sov. Phys. JETP **63**, 613 (1986)